

Correlation Between Probe Shape and Atomic Friction Peaks at Graphite Step Edges

Yalin Dong · Xin Z. Liu · Philip Egberts ·
Zhijiang Ye · Robert W. Carpick · Ashlie Martini

Received: 30 September 2012 / Accepted: 14 November 2012 / Published online: 30 November 2012
© Springer Science+Business Media New York 2012

Abstract Molecular dynamics simulation and atomic force microscopy are used to study the nature of friction between nanoscale tips and graphite step edges. Both techniques show that the width of the lateral force peak as the probe moves up a step is directly correlated with the size and shape of the tip. The origin of that relationship is explored and the similarities and differences between the measurements and simulations are discussed. The observations suggest that the relationship between lateral force peak width and tip geometry can be used as a real-time monitor for tip wear during atomic scale friction measurements.

Keywords Molecular dynamics (MD) simulation · Atomic force microscopy (AFM) · Atomic friction

1 Introduction

The surfaces of ordered materials are well-known to exhibit atomic-scale steps where an uppermost layer of atoms begins or ends. Atomic force microscopy (AFM) measurements of such steps have revealed that they can

significantly affect friction. As the AFM tip slides up a step, measurements consistently show an enhanced lateral force resisting motion [1–4]. This observation has been reported for various materials including highly ordered pyrolytic graphite (HOPG), Au(111), and NaCl(100), and under different measurement conditions ranging from ultra-high vacuum to ambient environments. The effect arises from both a geometric contribution and an enhanced friction force at the step edge, which work in concert to resist motion, thus leading to a clear increase in the lateral force in the vicinity of the step. When the AFM tip slides down a step, the lateral force can either increase or decrease compared to the lateral force on the terrace [3, 4]. These two possibilities are due to the opposing signs of the geometric (reducing the lateral force) and frictional (increasing the lateral force) contributions [4]; the net effect depends on the relative magnitude of these two contributions. In this study, we focus on the lateral forces observed while scanning up a step, due to the clear and consistent observation of an enhanced lateral force: a discussion of their relative magnitudes as determined by considering both upward and downward sliding will be published separately.

The lateral force peak due to a step edge contains substantial information about the material being measured as well as the origin of friction itself. To better understand the information available, here we investigate a specific feature, the width of the lateral force peak that occurs while scanning up atomic steps on a graphite surface. Graphite is chosen because it exhibits well-defined atomic steps, is chemically stable, and has been widely used to investigate the underlying mechanisms of atomic friction including the first measurement of atomic-stick slip [5], observation of structural superlubricity [6], friction enhancement when only a few (or one) sheet is present [7], and many others.

Y. Dong (✉)
School of Mechanical Engineering, Purdue University,
West Lafayette, IN, USA
e-mail: yann.dong@gmail.com

X. Z. Liu · P. Egberts · R. W. Carpick
Department of Mechanical Engineering and Applied Mechanics,
University of Pennsylvania, Philadelphia, PA, USA
e-mail: carpick@seas.upenn.edu

Z. Ye · A. Martini
School of Engineering, University of California Merced,
Merced, CA, USA
e-mail: amartini@ucmerced.edu

Graphite is also an ideal material from a modeling perspective because its structure is well-defined, and validated empirical potentials are available to describe its interatomic interactions.

In this study, we use AFM measurements complemented by molecular dynamics (MD) simulations to investigate friction at graphite step edges. The experiments provide a quantitative measure of how steps affect friction. The simulations allow direct access to the buried interface and thus provide an atomic-level picture of the origin of that friction. While similar experiments have shown the enhancement of lateral forces at atomic step edges [1–4], only a few studies have reported features of that lateral force having dimensions corresponding to the size of the AFM tip-sample contact [4, 8]. In this paper, we investigate this correlation further experimentally and through the first fully atomistic study of lateral forces at a step edge. The results obtained from both techniques, AFM and MD, show that there is a direct relationship between the width of the lateral force peak at the step and the size and shape of the tip. We explore the origin of that relationship as well as the similarities and differences between the measurements and model predictions. Finally, we suggest a potential application for this study where the relationship between peak width and tip geometry can be used as a real-time monitor for tip wear during atomic scale friction measurement.

2 Methodology

2.1 AFM Experiments

Two AFM's were used for the experiments. A RHK 350 AFM (RHK Technology) was used under environmental conditions, where the main chamber was purged with clean, evaporated nitrogen gas (relative humidity <2%). The second system, an RHK 750 AFM (RHK Technology), was operated under high vacuum conditions at pressures of approximately 1×10^{-8} Torr. Silicon contact mode AFM probes (PPP-CONT, Nanosensors Inc.) were used in all experiments. The normal bending stiffness of these probes is typically ~ 0.2 N/m. The normal spring constant was calibrated using the Sader method [9], and the lateral bending stiffness was determined geometrically [10]. The sensitivity of the photodetector, allowing for the conversion of volts to nanometers, was determined by measuring the slope of the cantilever deflection signal in a force-distance curve. Samples were prepared by cleaving highly ordered pyrolytic graphite (HOPG), purchased from SPI (SPI Supplies Inc., USA). Following cleaving, samples were inserted into the AFM chamber within a few seconds.

Step edges were selected based on their orientation with respect to the fast scan direction of the AFM cantilever,

i.e., we only examined monatomic steps that were oriented at 60° – 90° relative to the fast scan direction. This choice was made to maximize torsional twisting and minimize the longitudinal bending/buckling of the cantilever as the tip traveled over the step edge. We define the lateral force as the calibrated twisting signal of the cantilever measured as the tip slides over the surface. Lateral force signals were collected as the AFM probe scanned across the step edge. *Post-mortem* transmission electron microscopy (TEM) images of the tips were acquired following AFM measurements using a field-emission TEM (JEOL 2010F), and are, therefore, representative of the tip shape at the end of the AFM experiment. The region of the very end of the tip presumed to be in contact with the sample was traced and then fit to a spherical profile from which a curvature radius was extracted. The cantilever tilt (22.5° as specified by the manufacturer) was taken into account when tracing the contacting asperity of the tip apex. Analysis of AFM images has been performed with the WSxM software [11].

2.2 MD Simulation

The atomistic model is shown in Fig. 1. The model consists of a diamond tip and a three-layer graphite substrate. The topmost graphite sheet extended laterally only half of the length of the other two sheets in the sliding direction. In the simulation, the tip moves from left to right so that it steps up from the middle graphene sheet to the topmost graphene sheet. To simulate feedback control in AFM experiments, we scanned the tip over the surface with a constant force, allowing the z -position of the tip to change naturally as it traverses the step edge. Ideal graphite steps can either be arm chair or zigzag terminated. Although it has been reported that the termination type has a significant effect on electronic properties [12], these properties were not captured in the atomistic simulations, and we did not observe an effect on friction. All results shown in this paper correspond to the zigzag configuration.

Several different tip shapes and sizes were modeled. The default shape was hemispherical with radii of curvature varying from 2 to 7 nm. In addition, we performed simulations with truncated hemispheres to capture the effect of tip wear (discussed later). To accommodate tips with different radii, the size of the substrate was also varied; the substrate must be large enough to ensure that periodic images of the substrate do not interact with the tip, but small enough to be computationally efficient. Boundaries were periodic in the x -direction, free in the z -direction, and either a fixed or free boundary in the y -direction to enable investigation of the effect of the boundary condition.

The bottom layer of the substrate and the top five layers of the tip were treated as rigid bodies. The rigid atoms of the tip were pulled laterally across the step edge by a support moving

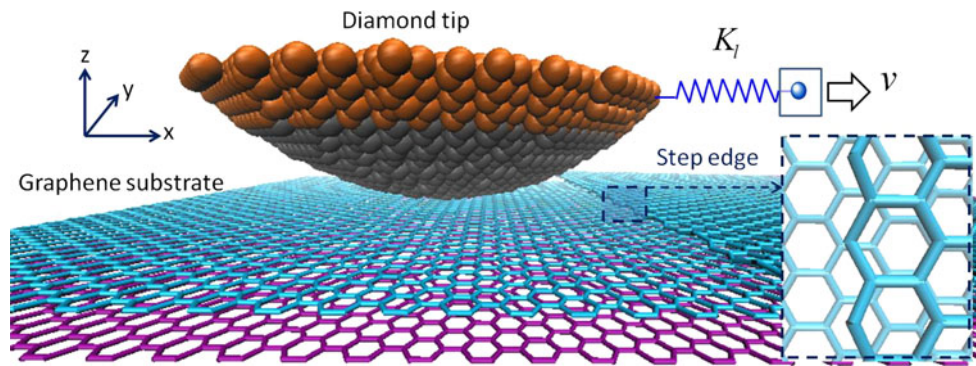


Fig. 1 Snapshot of the molecular dynamics simulation in which a model tip slides from left to right, or in the step-up direction, over a graphite substrate. The stiffness of the cantilever is mimicked by a

harmonic spring with lateral stiffness K_l through which the support, moving with constant speed v , pulls the tip along the substrate. A close-up of the zigzag step edge is shown in the inset.

at a constant speed v of 2 m/s. The tip atoms and the support were connected through a harmonic spring with a lateral stiffness K_l of 4 N/m that acts in the parallel to the surface; this falls in the range of the total lateral stiffness measured in AFM, which were found to be 6 ± 3 N/m depending on the tip. A constant normal load was applied directly to the top rigid layers of the tip. Normal loads ranging from -10 nN to 10 nN were applied in the simulation. A Langevin thermostat [13] was applied to the non-fixed atoms to keep the temperature of the system at approximately 300 K. The AIREBO [14] potential, which is known to be able to describe the mechanical properties of short distance C–C bonds as well as the long distance van der Waals force, was employed to govern the interaction of atoms within the tip and substrate. The interaction between the tip and substrate was simulated by the Leonard-Jones (LJ) potential with parameters adopted from Ref. [14] as well. The LJ potential was used here based on the assumption that the surface of the AFM tip is likely passivated (for example, by hydrogen) during sliding experiments, so that the interaction between tip and substrate is not chemical in nature. For computational efficiency, we did not explicitly model passivating species on the surface of the tip. Simulations were carried out using the molecular dynamics simulation package LAMMPS [15].

3 Results

3.1 Unworn/Spherical Tip

In this section, we describe the results of AFM measurements with unworn tips and MD simulations of perfectly hemispherical tips. The tip size (radius) will then be correlated with the width of the enhanced lateral force observed at the steps edge.

Figure 2a, b show examples of the lateral force typically observed when the tip slides up a monatomic step edge

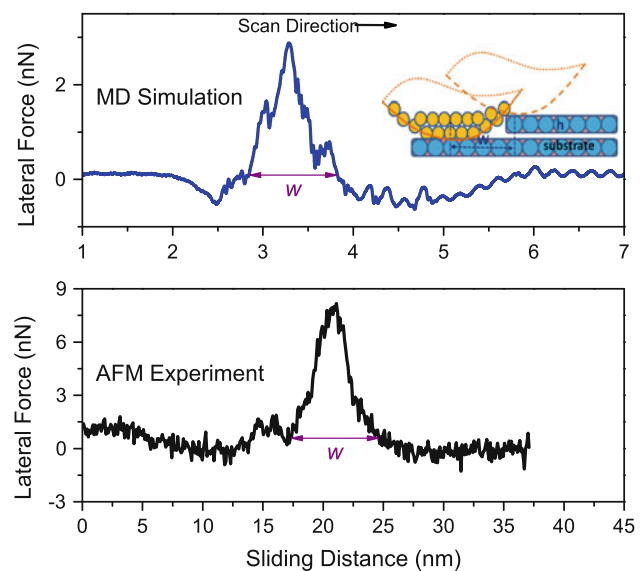


Fig. 2 **a** A typical lateral force profile obtained from MD simulation with a hemispherical tip radius of 4 nm at an applied load of 0 nN. A peak in the lateral force whose width is labeled as w is observed at a sliding distance of approximately 3.5 nm. The inset illustrates the tip's trajectory over the surface with a geometric drawing showing the relationship between the tip, the peak width w , and the height h of the graphite step. **b** A representative lateral force profile from an AFM experiment where the tip slides in the step up direction acquired at an applied load of 2 nN. As for the result from MD simulation, the width of the lateral force peak at the step is identified by w .

from a MD simulation and an AFM experiment, respectively. To the right of the peak in Fig. 2a, the force exhibits the regular saw-tooth pattern with atomic lattice periodicity characteristic of atomic stick-slip. Although not seen in the AFM data at this scale, high resolution experimental images consistently reveal stick-slip behavior with the lattice periodicity as well. Clearly, in both the experiment and simulation, the width of the lateral force peak at the step edge w , defined as the distance from one side of the peak to the other at the mean lateral force on the terrace, is much

larger than the 0.28 nm period of the stick-slip pattern. The mismatch between the lateral dimensions of atomic stick-slip and the width of the force peak at the step edge suggests that the size of the latter is related to the tip as opposed to the periodicity of the substrate lattice.

To examine the correlation between lateral force peak width and tip size, we perform the same simulation using hemispherical tips with different radii. We observe a monotonic increase of peak width with tip radius (Fig. 3). This result is consistent with the hypothesis that the width of the lateral force peak across a step is directly related to the size of the tip.

We further verify the correlation between step width and tip radius using AFM measurements. Five different Si tips are shown in the insets of Fig. 4. The radius of each tip and the width of the corresponding lateral force peak were determined. The variation of peak width with radius in Fig. 4 shows the same trend as the simulations: a larger tip radius leads to a larger measured lateral force peak width. Thus the MD simulations and AFM experiments show the same qualitative behavior. We note that, consistent with extensive observations of commercial AFM tips, the overall tip shapes exhibit irregularities. However, for all tips presented here, a lowest asperity could be clearly identified and fit to a spherical profile.

3.2 Worn/Truncated Tip

In this section we explore the effect of tip evolution on friction at a step edge. Specifically, we characterize the lateral force peak width measured by the same tip as it

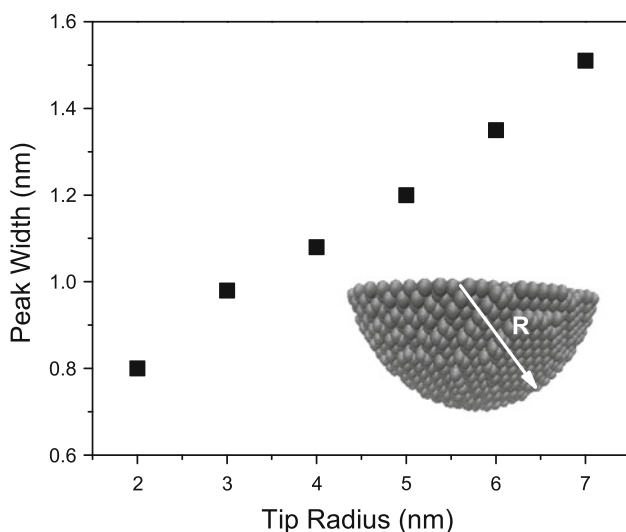


Fig. 3 Simulation-predicted width of the lateral force peak as a function of tip radius. A snapshot of a hemispherical tip with a radius of $R = 4$ nm is shown in the inset. Measurements of the peak width shown here are acquired at an applied load of 0 nN and using free boundary conditions in the y -direction.

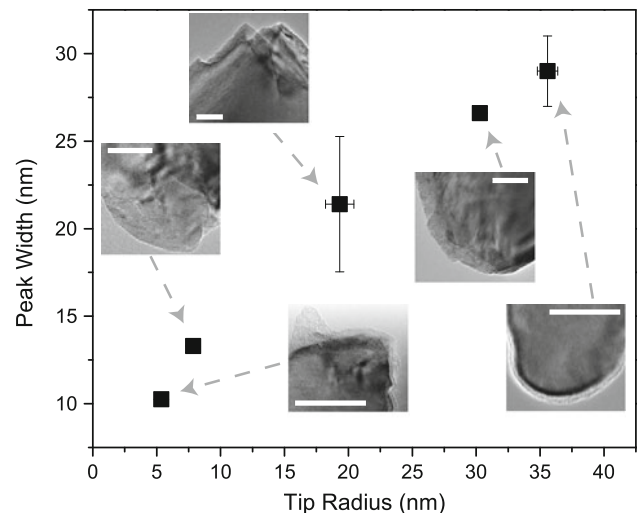


Fig. 4 Experimentally measured friction peak width as a function of tip radius. *Post-mortem* TEM images for each measurement are shown as insets. All tips were used in the UHV-AFM system except for the smallest tip, which was used in the environmental system. Measurements were acquired in contact mode at a constant applied load of 2.0 ± 0.5 nN. White lines in the inset TEM images correspond to 40 nm.

wears over time, and of model tips that are truncated to mimic the wear process.

Wear studies of AFM tips have shown that the tip apex often becomes flattened while scanning flat surfaces [16]. We mimic this effect with truncated tips where the lowest atomic layers of the hemispherical tip are removed. The top-left inset of Fig. 5 shows the tip shape with varying degrees of truncation where greater truncation is intended to capture the effect of more wear. We find that the lateral force peak width increases monotonically with truncation as shown in Fig. 5; the inset shows representative lateral force traces.

A comparable experimental result is given in Fig. 6, which shows the change in the lateral force peak width as a tip is repeatedly scanned up a step. We observe a monotonic increase in peak width with total scan distance. The rate of that increase is faster at the beginning of the experiment. Based on the results of the truncated tip simulations, the experimentally observed increase in peak width is likely attributable to a flattening of the tip. An increased bluntness was also suggested by the quality of the topographic images obtained during these measurements since sharper tips are able to generate higher resolution topographic images [16, 17]. However, direct measurement of the evolving tip shape was not performed for this experiment as it would have required repeatedly interrupting the scanning to obtain TEM images, or AFM-based blind tip reconstruction measurements on another sample. Regardless, from Fig. 6, we can infer that the initial rapid increase in the force peak width is due to the high wear rate associated with the

extremely sharp initial tip shape, occurring while contact stresses are the highest. After initial wear, the slope of the width versus sliding distance curve is relatively constant corresponding to a steady-state wear rate. This observation is consistent with other reports of tip wear, where initially high wear rates have been observed for sharpened AFM tips with similar shapes and sizes as those used here [16].

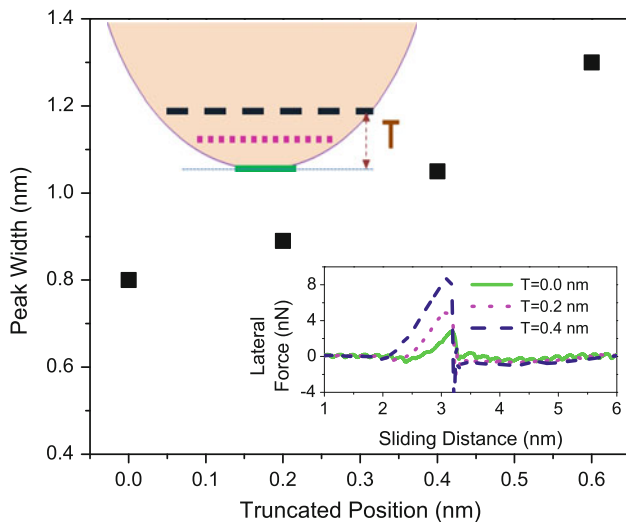


Fig. 5 Results from MD simulations showing lateral force peak width for a 2 nm radius tip versus an increasing degree of truncation. The truncation is illustrated geometrically by the schematic in the upper-left inset. In the bottom right inset, three representative lateral force traces are given to graphically show the change in lateral force profile with increasing truncation. All measurements shown in this figure were acquired at an applied load of 0 nN with fixed boundary conditions.

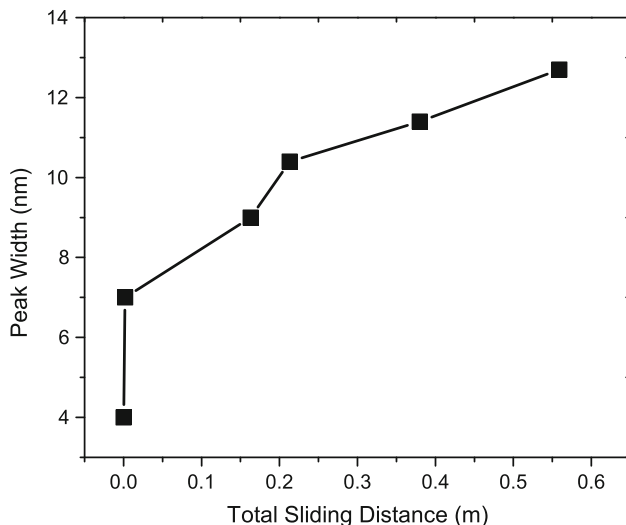


Fig. 6 Step width variation with sliding distance measured in the environmental AFM. The initial tip radius was 24 ± 5 nm based on blind tip reconstruction (BTR) conducted on a Nioprobe surface using the BTR function of SPIP (Image Metrology Inc., Denmark). The normal load was 0.9 nN throughout the tip wear measurement

4 Discussion

4.1 Comparison Between Simulation and Experiment

Both the experimental measurements and simulations have shown that the width of the lateral force peak when a tip moves up a step increases with increasing tip size and bluntness. However, despite the consistency of these trends, quantitative comparison of Figs. 3 and 4 reveals that the measured peak width is significantly larger than that predicted by the simulation. For example, with a 5 nm radius, the simulation-predicted width is 1.2 nm while the experimentally measured width is 10 nm. In this section we will explore the sources of this difference.

If the enhanced friction were purely geometric in origin (i.e., assuming smooth, rigid, non-adhesive continuum materials in contact), then we can estimate that the width of the peak should be $w = \sqrt{2Rh}$ where R is the tip radius and h is the height of the step (for a one-layer graphene step this is 0.335 nm). The geometric analysis, therefore, predicts a peak width of 1.8 nm for the 5 nm radius tip; this prediction is slightly greater than that observed in simulations and significantly less than that observed in experiments as shown in Fig. 7. The small discrepancy with the simulations can be explained by the tip hopping up the step before it reaches the geometrically defined limit due to attractive forces at the step, or by a slight decrease in h as the tip elastically compresses the step. Both of these are observed to occur in the simulations. The primary question that remains then is why the experimentally measured widths are so much larger than those predicted geometrically or by the atomistic simulation. To address this

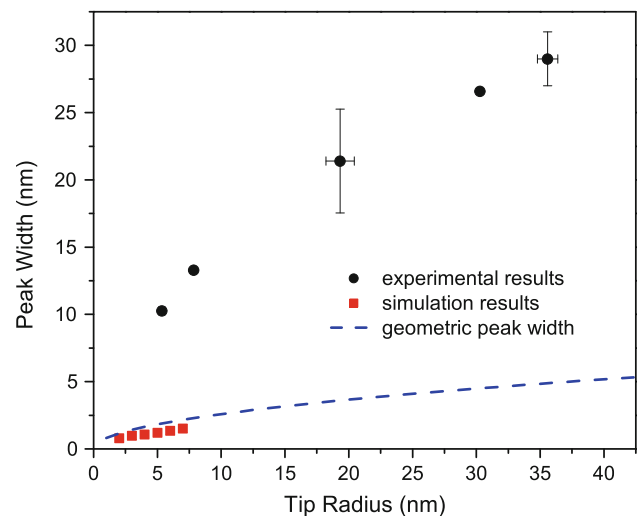


Fig. 7 Lateral force peak width versus tip radius from the MD simulation (squares), AFM experiment (circles), and an analytical expression (dashed line) based on the assumption that the step provides only geometric resistance to sliding

question, we have examined the effect of various simulation parameters. As will be discussed in the following paragraphs, we explored the effects of tip deformation, normal load, lateral stiffness, sliding angle, and substrate deformation.

One possible reason for the quantitative gap in measured lateral force width is that the MD simulation assumes the tip to have an ideal hemispherical shape. In experiments, however, such an ideally shaped tip is rare because of the long sliding distances experienced by the tip before finding an area of interest which, as discussed previously, can result in blunting. In addition, the sharpening process used to make silicon tips often results in non-ideal tip apex shapes. The TEM images of tips used to obtain the data in Fig. 4 suggest that the apex was relatively hemispherical. However, since these images were taken after the friction measurements, we cannot exclude the possibility that varying local imperfections or non-uniform elastic deformation of the contact occurred during sliding. In addition, TEM provides only a 2-dimensional profile which means that a tip that appears round in one plane may be quite flat in another. The simulations showed that the lateral force peak width increases with truncation (Fig. 5). Therefore, it may be that large experimentally measured widths were caused by flattening that occurred during sliding but was not present or not captured by the post-sliding TEM measurements. Tip deformation during sliding is not observable in the simulations of a diamond tip which deforms very little under the loading conditions explored in this study. However, the rate of increase of the lateral force peak width with the degree of truncation predicted by the simulations is relatively small, which indicates that elastic AFM tip deformation alone cannot explain the large experimentally measured widths.

Another potential contribution may be associated with applied load. It has been shown experimentally that increasing normal force will increase the height of the peak lateral force at a step edge [3]. We, therefore, considered the possibility that increasing load might also affect the width of that peak. We have examined the effect of normal force in both simulation (from -10 to $+10$ nN) and experiment (from -20 to $+20$ nN) and found no observable trend in the variation of the peak width.

It is well-known that a reduced lateral stiffness can cause an increase in multiple slips as the tip slides over an atomically flat surface [18–21]. The energy barrier imposed by the step edge is analogous to the energy barrier formed by discrete atoms on a flat surface, but having a much larger magnitude. As such, a lower lateral contact stiffness requires a greater sliding distance to reach the necessary force to traverse this potential barrier. Thus, a wider lateral force peak is observed with more compliant contacts. In this case, the build up of lateral force required by the tip to

move forward remains constant, but the support must travel further if the contact is more compliant to reach that same force, thus giving the appearance of a wider force peak. Contact compliance is affected by both the probe and the substrate. We explored the potential effect of probe compliance using simulations with lateral spring stiffness ranging from 0.5 to 10 N/m. These simulations showed that the lateral peak width does increase with decreasing spring stiffness. However, we observed another effect, whereby decreasing the lateral spring stiffness caused the drop in lateral force just after the tip traverses the step edge to be sharper. This is inconsistent with most of our AFM measurements where the lateral force at step edge drops gradually. Therefore, we conclude that a soft lateral spring, although able to generate larger lateral force peak widths, is likely not representative of the experimental conditions. Compliance of the substrate itself may also play a role. In fact, one reason that the peak widths reported in another experimental study [4] were so much smaller than those reported here could be because the shear modulus for strain along the basal plane of NaCl (001) is larger (12.81 GPa [22]) than that of graphite (0001) (3.96 GPa [23]). We attempted in the simulations to decrease the compliance of the graphite normal to the surface by adding more substrate layers [7], but it was found to have a negligible effect on lateral force peak width.

We also investigated the effect of the angle of the step edge relative to the sliding direction. In AFM measurements, it is often difficult to perfectly align the crystal orientation and the step direction with respect to the geometry of the cantilever. To measure friction and to obtain the best topographic image, the step should be perpendicular to the fast scan direction of the AFM as well as the long axis of the cantilever, which is not possible to realize perfectly. To evaluate this effect in the simulation, we measured the lateral force peak width as the sliding direction was changed from 45° to 90° . We observed almost no change in width indicating that angle cannot explain the difference between experiment and simulation.

Another factor which could contribute to the difference between simulation and experiment arises from the relatively weak bonding between graphene layers. Weak interlayer interactions can contribute to wear of the graphite during the reciprocating motion of the AFM tip. Typically this wear is observed as a ripping or tearing of individual graphene sheets or folding over/rolling up of a graphene sheet at a step edge [24]. Wear on graphite surfaces can be observed when an AFM tip slides over the surface at high loads or when the interaction between the tip and sample is stronger than the interlayer forces between the graphene layers. We do not model conditions extreme enough to cause actual wear of the graphite. However, we do observe that large truncated tips compress

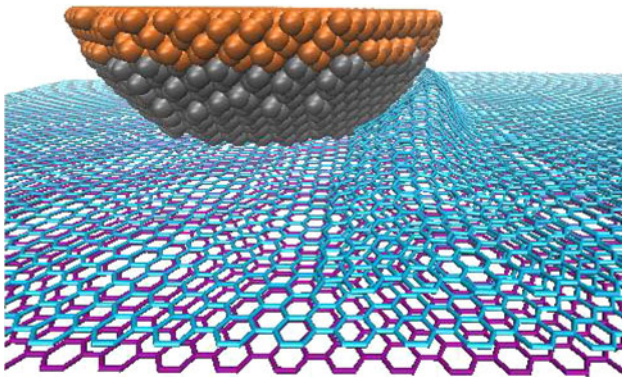


Fig. 8 Snapshot of a model truncated tip ($R = 3$ nm, $T = 0.4$ nm) sliding up the graphite step with free boundary conditions in the y -direction. We observed significant compression of the step before the tip slips forward over the step edge.

the uppermost graphene layer before moving up the step. Figure 8 shows a snapshot taken of a typical MD simulation just before a truncated tip traverses the step edge. The effect of this compression is that the tip, restrained by the upper layer, moves up the step edge later than it otherwise would if it were not compressed, and, therefore, the force peak is correspondingly wider. In the simulations, we can control this behavior to some degree through the boundary conditions. The two limiting cases we explored were fixed (upper layer perimeter atoms cannot move) and free (no constraints on upper layer graphite atoms) boundaries in the y -direction (perpendicular to the sliding direction, in the plane of sliding). For small tips, the boundary conditions had no significant effect and for these cases we used free boundary conditions. However, for truncated tips, we found that the free boundary condition resulted in more compression or even roll-up of the step edge. In some cases, large or highly truncated tips pushed the graphene sheet forward, preventing the tip from surmounting the step altogether. For these cases, a fixed boundary condition had to be used. The simulated fixed and free boundaries (when free boundaries could be used) likely bracket the experimental case, where resistance to deformation at the step is due predominantly to the interaction between the top layer and those below it. Therefore, deformation of the step itself may partially explain the difference in lateral force peak width in experiment and simulation. Studies where this effect is carefully tested by significantly increasing the sample size to eliminate boundary effects are required to quantitatively compare this effect with experiments.

In summary, we considered the influence of tip deformation, load, spring/sample compliance, step angle, and graphene deformation using simulations and found no definitive evidence supporting any one of those properties/conditions as the sole source of the quantitative difference between simulation and experimental step-induced lateral

force peak widths. Deformation of the top layer of the graphite at the step edge in the form of wrinkling or roll-up was the only effect that had the potential for a substantial effect. Other possible factors that we cannot capture with our current simulation methods include chemical reactions at the step edge, effects due to the larger body of the tip (as opposed to the tip apex which is described by the model), unsaturated bonds at the tip apex produced by wear, chemical groups or third bodies present at the step, or an electric field caused by the difference between the work functions of the tip and substrate. These effects are difficult to verify experimentally. Therefore, to explain the quantitative difference between simulation and experiment, we are left with the possibilities that (a) a factor we cannot capture in the simulation is the major cause, or (b) the difference is attributable to deformation of the step, which we can only partially capture in the simulation due to size limitations.

4.2 Real-Time Tip Wear Monitor

We have shown that there is a direct correlation between tip size and shape and the width of the lateral force peak that arises at an atomic step edge. We now suggest a practical application for this observation.

The resolution of an AFM is significantly affected by the tip size and shape. However, when imaging the surface in contact mode, sharp silicon AFM probes often experience wear, severely affecting the resolution attainable during long-term measurements [25–28]. Different methods have been proposed to avoid tip wear and degradation, such as AFM cantilevers with integrated tips made from diamond [29]. However, the sharpest probes are still manufactured from silicon, and have a proven track record for achieving lattice resolution in contact mode, or even atomic resolution in some cases [30]. Characterizing the evolution of a tip is, therefore, important to interpreting the measurements taken using that tip.

There are several existing techniques used to characterize the AFM tips. These include blind tip reconstruction [31, 32], use of another sharper AFM tip [25], tip characterizers with well-fabricated patterns or sharp features on their surfaces [33, 34], or advanced imaging techniques such as TEM, used before and after the scanning [16]. Most of these techniques cannot be used in situ and thus in real time. Real-time characterization of the tip is challenging because the tip apex is nanoscale in size, it is buried at the interface during measurement, and it may experience wear which changes its shape. One very promising technique is in situ TEM. However, considering its sophistication and expense, access to such facilities is limited. Therefore, a simpler alternative for real-time tip monitoring would be extremely useful.

Atomic step edges are ubiquitous on atomically flat surfaces, and we have shown in this paper that there is a direct correlation between tip size/shape and the width of the lateral force peak that arises at a step. We propose that this correlation can be used as a simple, but effective way to estimate in situ the evolution of the tip. Our measurements have shown that the geometric relationship between peak width, step height, and tip radius underestimates the experimentally measured width. If we assume that whatever factor or factors F causing that underestimation are not related to radius or height, we can write, $w = F\sqrt{2Rh}$ where F is a dimensionless correction factor to the equation for non-adhesive interactions between a rigid round tip and a rigid step. Fitting this equation to our experiments gives $F = 5.9$, but we do not assign a specific physical meaning to this term here. If two different steps (whose height can be confirmed using AFM topography measurements) are encountered during a scan, the *change* in a measured lateral force peak width can be directly correlated to an effective radius of the worn tip, $\Delta R \propto \Delta w^2$. In other words, monitoring the width of lateral force peaks at atomic steps can be used as a real-time measure of the evolution of the tip. To realize its potential, this approach needs to be thoroughly vetted through a focused study on AFM tip evolution.

5 Conclusion

We have used AFM experiments and MD simulation to explore the lateral force that arises as an AFM tip scans up a graphite step edge. First, we analyzed the results of AFM measurements with unworn tips and MD simulations of perfectly hemispherical tips, and found that the width of the lateral force peak at the step increases monotonically with tip size. Then, we explored the effect of tip changes by characterizing the lateral force peak width measured by one tip as it scans long distances in the experiments. We compared this with simulations of model tips that are truncated to mimic the wear process. These results showed that the lateral force peak width increases with total measurement distance in the experiment, and with the degree of tip truncation in the simulation; based on this, the increase with measurement distance in the experiment was interpreted as resulting from blunting of the tip through wear. Next, we discussed the larger peak widths observed experimentally compared with the simulations. Although tip wear occurs during the measurements, we rule out changes in the tip's size due to wear as the cause of the discrepancy since the tip size was measured *post-mortem* using TEM. We then concluded that, except for step deformation, none of the other effects explicitly captured using MD simulation were likely

to have an effect on width substantial enough to explain the observed difference. In other words, these findings suggest that the difference is due to either an effect not described in the model, or to deformation of the top layer of graphite at the step edge since the simulations suggest that this effect could contribute to the difference. Finally, we propose an application for the relationship between tip size and lateral force peak width in which measuring the peak width while scanning up steps of known height might be used as a real-time monitor of tip wear.

Acknowledgments The authors would like to thank the U.S. National Science Foundation for its support through Grants No. CMMI 1068552 and CMMI-1068741. We are grateful to Dr. Hendrik Hölscher and Dr. Qunyang Li for the insightful discussions when initiating this work and to Tevis D. B. Jacobs and Graham Wabiszewski for their help to acquire TEM images. P.E. would like to acknowledge financial support from the Natural Sciences and Engineering Research Council (NSERC) of Canada.

References

- Müller, T., Lohrmann, M., Kässer, T., Marti, O., Mlynek, J., Krausch, G.: Frictional force between a sharp asperity and a surface Step. *Phys. Rev. Lett.* **79**(25), 5066 (1997)
- Hausen, F., Nielinger, M., Ernst, S., Baltrusch, H.: Nanotribology at single crystal electrodes: influence of ionic adsorbates on friction forces studied with AFM. *Electrochimica Acta* **53**(21), 6058 (2008)
- Hölscher, H., Ebeling, D., Schwarz, U.: Friction at atomic-scale surface steps: experiment and theory. *Phys. Rev. Lett.* **101**(24), 246105 (2008)
- Steiner, P., Gnecco, E., Krok, F., Budzioch, J., Walczak, L., Konior, J., Szymonski, M., Meyer, E.: Atomic-scale friction on stepped surfaces of ionic crystals. *Phys. Rev. Lett.* **106**(18), 186104 (2011)
- Mate, C., McClelland, G., Erlandsson, R., Chiang, S.: Atomic-scale friction of a tungsten tip on a graphite surface. *Phys. Rev. Lett.* **59**(17), 1942 (1987)
- Dienwiebel, M., Verhoeven, G., Pradeep, N., Frenken, J., Heimberg, J., Zandbergen, H.: Superlubricity of graphite. *Phys. Rev. Lett.* **92**(12), 126101 (2004)
- Lee, C., Li, Q., Kalb, W., Liu, X., Berger, H., Carpick, R., Hone, J.: Frictional characteristics of atomically thin sheets. *Science* **328**(5974), 76 (2010)
- Filleter, T., Paul, W., Bennewitz, R.: Atomic structure and friction of ultrathin films of KBr on Cu(100). *Phys. Rev. B.* **77**(3), 035430 (2008)
- Green, C., Lioe, H., Cleveland, J., Proksch, R., Mulvaney, P., Sader, J.: Normal and torsional spring constants of atomic force microscope cantilevers. *Rev. Sci. Instrum.* **75**, 1988 (2004)
- Young, W.: *Roark's Formulas for Stress and Strain*. 6 edn. McGraw-Hill, New York (1989)
- Horcas, I., Fernandez, R., Gomez-Rodriguez, J., Colchero, J., Gómez-Herrero, J., Baro, A.: WSXM: a software for scanning probe microscopy and a tool for nanotechnology. *Rev. Sci. Instrum.* **78**(1), 013705 (2007)
- Niimi, Y., Matsui, T., Kambara, H., Tagami, K., Tsukada, M., Fukuyama, H.: Scanning tunneling microscopy and spectroscopy of the electronic local density of states of graphite surfaces near monoatomic step edges. *Phys. Rev. B.* **73**(8), 085421 (2006)

13. Schneider, T., Stoll, E.: Molecular-dynamics study of a three-dimensional one-component model for distortive phase transitions. *Phys. Rev. B* **17**(3), 1302 (1978)
14. Stuart, S., Tutein, A., Harrison, J.: A reactive potential for hydrocarbons with intermolecular interactions. *J. Chem. Phys.* **112**, 6472 (2000)
15. Plimpton, S.: Fast parallel algorithms for short-range molecular dynamics. *J. Comput. Phys.* **117**(1), 1 (1995)
16. Liu, J., Notbohm, J., Carpick, R., Turner, K.: Method for characterizing nanoscale wear of atomic force microscope tips. *ACS Nano* **4**(7), 3763 (2010)
17. Liu, J., Grierson, D.S., Moldovan, N., Notbohm, J., Li, S., Jaroenapibal, P., O'Connor, S.D., Sumant, A.V., Neelakantan, N., Carlisle, J.A., Turner, K.T., Carpick, R.W.: Preventing nanoscale wear of atomic force microscopy tips through the use of monolithic ultrananocrystalline diamond probes. *Small* **6**(10), 1140 (2010)
18. Johnson, K., Woodhouse, J.: Stick-slip motion in the atomic force microscope. *Tribol. Lett.* **5**(2), 155 (1998)
19. Socoliuc, A., Bennewitz, R., Gnecco, E., Meyer, E.: Transition from stick-slip to continuous sliding in atomic friction: entering a new regime of ultralow friction. *Phys. Rev. Lett.* **92**(13), 134301 (2004)
20. Medyanik, S., Liu, W., Sung, I., Carpick, R.: Predictions and observations of multiple slip modes in atomic-scale friction. *Phys. Rev. Lett.* **97**(13), 136106 (2006)
21. Dong, Y., Vadakkepatt, A., Martini, A.: Analytical models for atomic friction. *Tribol. Lett.* **44**(3), 367 (2011)
22. Hunter, L., Siegel, S.: The variation with temperature of the principal elastic moduli of NaCl near the melting point. *Phys. Rev.* **61**, 84 (1942)
23. Grimsditch, M.: Shear elastic modulus of graphite. *J. Phys. C.* **16**(5), 143 (1983)
24. Ebbesen, T.W., Hiura, H.: Graphene in 3-dimensions: towards graphite origami. *Adv. Mater.* **7**(6), 582 (1995)
25. Khurshudov, A., Kato, K.: Wear of the atomic force microscope tip under light load, studied by atomic force microscopy. *Ultramicroscopy* **60**(1), 11 (1995)
26. Agrawal, R., Moldovan, N., Espinosa, H.: An energy-based model to predict wear in nanocrystalline diamond atomic force microscopy tips. *J Appl. Phys.* **106**, 064311 (2009)
27. Jacobs, T., Gotsmann, B., Lantz, M., Carpick, R.: On the application of transition state theory to atomic-scale wear. *Tribol. Lett.* **39**(3), 257 (2010)
28. Killgore, J.P., Geiss, R.H., Hurley, D.C.: Continuous measurement of atomic force microscope tip wear by contact resonance force microscopy. *Small* **7**(8), 1018 (2011)
29. Kim, K.-H., Moldovan, N., Ke, C., Espinosa, H.D., Xiao, X., Carlisle, J.A., Auciello, O.: Novel ultrananocrystalline diamond probes for high-resolution low-wear nanolithographic techniques. *Small* **1**(8-9), 866 (2005)
30. Maier, S., Gnecco, E., Baratoff, A., Bennewitz, R., Meyer, E.: Atomic-scale friction modulated by a buried interface: combined atomic and friction force microscopy experiments. *Phys. Rev. B* **78**(4), 045432 (2008)
31. Dongmo, S., Troyon, M., Vautrot, P., Delain, E., Bonnet, N.: Blind restoration method of scanning tunneling and atomic force microscopy images. *J. Vac. Sci. Tech. B* **14**(2), 1552 (1996)
32. Dongmo, L., Villarrubia, J., Jones, S., Renegar, T., Postek, M., Song, J.: Experimental test of blind tip reconstruction for scanning probe microscopy. *Ultramicroscopy* **85**(3), 141 (2000)
33. Bykov, V., Gologanov, A., Shevyakov, V.: Test structure for SPM tip shape deconvolution. *Appl. Phys. A.* **66**(5), 499 (1998)
34. Itoh, H., Fujimoto, T., Ichimura, S.: Tip characterizer for atomic force microscopy. *Rev. Sci. Instrum.* **77**(10), 103704 (2006)